Effect of Polymer Coatings from CO_2 on Water-Vapor Transport in Porous Media

Florence E. Hénon and Ruben G. Carbonell
Kenan Center for the Utilization of CO_2 in Manufacturing,
Dept. of Chemical Engineering, North Carolina State University, Raleigh, NC 27695

Joseph M. DeSimone
Kenan Center for the Utilization of CO_2 in Manufacturing, Dept. of Chemical Engineering,
North Carolina State University, Raleigh, NC 27695
and
Dept. of Chemistry, University of North Carolina-Chapel Hill, Chapel Hill, NC 27599

A variety of perfluorinated polyethers were coated onto surfaces of marble, sandstone and limestone samples from solutions in supercritical carbon dioxide. These polymers make ideal protectants for civil infrastructure by making stone surfaces hydrophobic and preventing penetration and deterioration of the stone by acid rain. The effective diffusivities of water vapor through coated and uncoated stones were measured as a function of polymer applied per unit area of sample. An analysis of the diffusive transport of water through the stones led to estimates of the penetration depths of the polymers and the percentages of blockage of the pores in the coated layers as a function of polymer surface coverage. Penetration depths were seen to strongly depend on the mean size and porosity of the stones. It is important for water-vapor diffusion to occur through the samples to prevent water condensation inside polymer-coated structural materials.

Introduction

Polymer coatings are often used for the protection of stone surfaces from environmental degradation. For this application, a polymer must satisfy specific requirements such as liquid-water repellence, transparency, and adequate aging rate, before being considered as a potential protective substance (Amoroso and Fassina, 1983; Price, 1996). The application of a polymeric film on the stone surface should reduce some degradation processes without enhancing others that could prove irreversible (Alessandrini et al., 1985; Ghigonetto, 1985). Most previous investigations have examined the physical and chemical properties of the stone and the polymer (Blaga and Yamasaki, 1986; Imbalzano et al., 1991; Jaroszynska and Kleps, 1986), but few studies have focused on the effect of polymer coatings on the transport properties of the stone (Littmann et al., 1993). These studies are important, as they help determine secondary effects of the coating materials, for example, the degree of pore blockage. Blockage of the pores by the polymer film can result in a reduction in the transport of gases through the stone, particularly water vapor. This reduction can cause water condensation and the accumulation of harmful agents inside the stone, resulting in increased deterioration of the material due to dissolution of minerals, growth of bacteria, exfoliation, cracks, and detachment of the underlying matrix (Ciarallo et al., 1985; Gauri, 1990; Young, 1996). For these reasons it is important to quantify the pore blockage resulting from the application of a polymeric coating on the stone surface and to understand its effect on the diffusion of water vapor through the porous medium.

The diffusion experiments presented in this article were conducted on three calcareous lithotypes commonly found in Italian architecture and greatly affected by today's polluted environment (Danin, 1993; Reddy et al., 1985; Sabbioni and Zappia, 1991; Wu, 1997). Samples of these stones were coated with three different perfluorinated polyethers with amide groups that have been proven effective protective polymers in the field of tone protection (Piacenti, 1994; Piacenti and Camaiti, 1994; Piacenti et al., 1993, 1992). Experiments were conducted to measure the reduction in water-vapor flux across

Correspondence concerning this article should be addressed to R. G. Carbonell.
Current address of F. E. Hénon: RF Micro Devices, 7628 Thorndike Road, Greensboro, NC 27409.

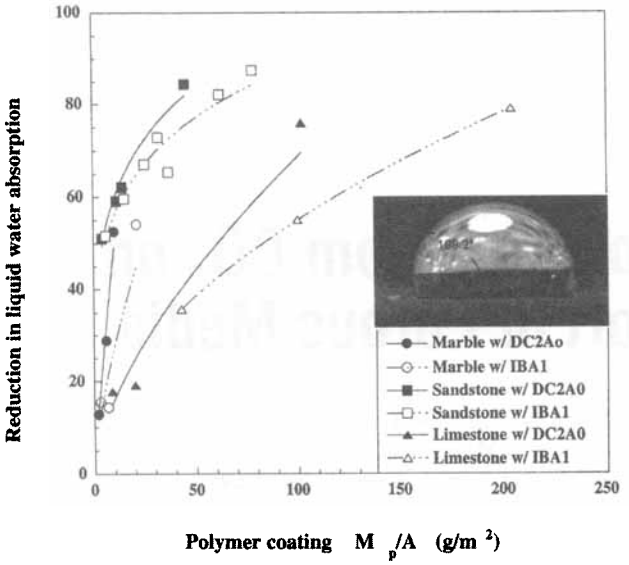

Figure 1. Reduction in liquid water absorption of fluorinated polymer coatings.

The side picture represents a liquid water droplet on sandstone sample S105 coated with 45 g/m^2 of DC2Ao.

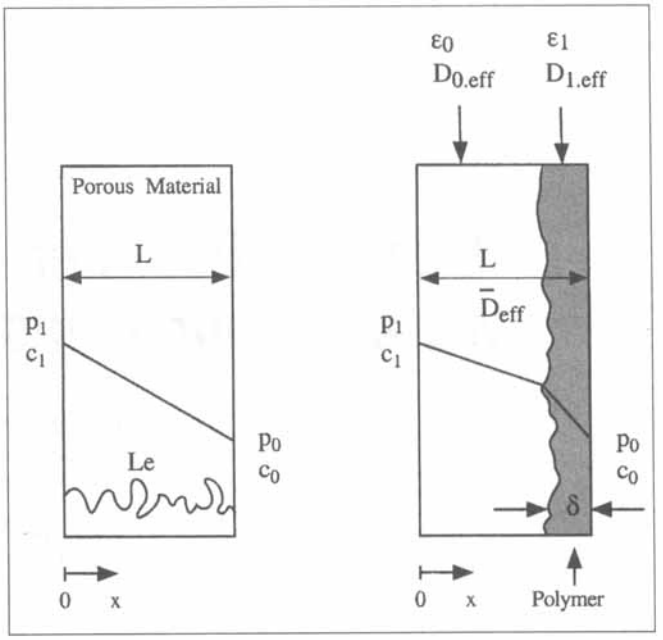

Figure 2. Coordinate system and nomenclature for one-dimensional steady-state diffusion in a porous medium.

the stone samples due to the application of fluorinated polymer coating on the surface of the stone substrates.

The polymers chosen are highly water-repellent and have been proven to reduce water absorption into stone by about 80% for at least 30 months (Matteoli et al., 1988). Measurements of the reduction in liquid-water absorption over a range of polymer coverage have also been performed in our laboratory. These results show a reduction in liquid-water absorption increasing from 20% to 90% for polymer coverage ranging from 4 g to 200 g of polymer per square meter of substrate (Figure 1).

Despite their many desirable characteristics for protection purposes, perfluoropolyethers have the major drawback of being soluble only in chlorinated fluorocarbons (CFCs), solvents that are widely responsible for the depletion of the ozone layer (Solomon et al., 1986). Potentially they could be applied in the form of an aqueous emulsion, but this would lead to nonuniform coatings, slow drying rates, and large amounts of contaminated water. To circumvent this problem, an environmentally benign solvent, carbon dioxide in its supercritical state, has been found (Kaiser, 1996; McHugh and Krukonis, 1994). Solubility measurements of several perfluoropolyethers, including the three studied in this article, IBAo, IBA1, and DC2Ao, have been carried out and are reported in Hénon et al. (1999). An atomization process from a supercritical CO_2 solution, achieved through the rapid expansion of supercritical solution (RESS) process, appears to be an appropriate method for the application of these protective materials. Details on the spraying device, the experimental procedure, as well as on a computational fluid dynamics code can be found in (Hénon et al., 1999). A patent has been filed on the use of this process for stone protection (Carbonell et al., 2000).

This article describes measurements of the flux of water vapor in natural (uncoated) stone and in the same stones coated with fluorinated polymers. One of the issues that this work addresses is the difference between coatings delivered from a supercritical carbon dioxide solution and coatings delivered from common liquid organic solvents. A wide range of polymer coverage up to 200 g/m^2 of substrate was investigated. From these measurements, the overall effective diffusivities of water vapor in the uncoated and coated samples were determined. The reduction in the effective diffusivity due to the application of a polymer coating on the stone was determined for the three lithotypes coated with three different polymers. An analysis of the water-vapor diffusion through the uncoated and the coated regions led to estimates of the penetration depth of the polymer in the porous medium and the percent reduction in the porosity of the stone in the coated layer. The penetration depth seems to be almost independent of polymer viscosity, indicating it might be controlled by a combination of capillary forces and/or gravitational forces acting on the polymer after its application on the stone from the RESS process.

Theory

Diffusion in porous media

When a sample of a porous material is subjected to two different gas-solute concentrations, c_0 and c_1 (partial pressures p_0 and p_1), but to equal total pressures and temperatures on either side, the solute flux through the porous sample will be due to diffusion only (Figure 2). At steady state, the local 1-D diffusive flux of the solute in the x-direction in the porous medium is given by (Bird et al., 1960)

$$< J > = - D_{\text{eff}} \frac{dc}{dx} = \text{constant} \qquad (1)$$

where D_{eff} is the effective diffusivity and dc/dx is the local solute concentration gradient in the substrate. The effective diffusivity is a function of the porosity, ϵ, and the tortuosity, τ, of the porous medium, as well as the diffusion coefficient D of the solute (Mason, 1983; Satterfield and Sherwood, 1963)

$$D_{\text{eff}} = \left(\frac{\epsilon}{\tau}\right) D \tag{2}$$

The tortuosity, τ, is defined as the ratio of the actual path length, L_e, that the molecule has to travel to get across the porous sample, to the sample thickness, L (Figure 2). The tortuosity, τ, is always greater than 1, and is in the order of $\sqrt{2}$ for unconsolidated materials (Carman, 1937; Satterfield and Sherwood, 1963). However, for consolidated materials like stone, τ can reach values that are considerably larger (Dullien, 1992; Satterfield and Sherwood, 1963).

The magnitude of the diffusion coefficient, D, in Eq. 2 varies with the Knudsen number, N_K, which determines the relative contribution from Knudsen and molecular diffusion (Geankoplis, 1993)

$$N_K = \frac{\lambda}{2\bar{r}} \tag{3}$$

Here $\bar{r}$ is the average radius of the pores of the medium, and λ is the mean free path of the diffusing species (Knudsen, 1934; Loeb, 1934)

$$\lambda = \frac{1}{\sqrt{2}\,\pi d^2 N} \tag{4}$$

The mean free path is controlled by the diameter, d, of the diffusing molecules (in our case water vapor), and the number of molecules per unit volume, N, in the gas phase.

For pores of average radius, $\bar{r}$, significantly larger than the mean free path of the diffusing molecules ($N_K \leq 0.01$), the diffusion process is controlled by molecular diffusion within the gas-filled pores; in this case, the diffusion coefficient is denoted by D_m and is only dependent on the temperature, pressure, and chemical composition of the gas phase (Present, 1958). On the other hand, if the pore diameters are smaller, or of the same order of magnitude as the mean free path ($N_K \geq 10$) the diffusion process is governed by collisions of the solute molecules with the walls of the pores (Knudsen diffusion) (Dullien, 1992). In this case, the diffusion coefficient, D, is then denoted by D_K and is a function of the pore radius in addition to the molecular weight of the diffusing species. For cylindrical pores, D_K can be estimated by the expression (Dullien, 1992; Geankoplis, 1993)

$$D_K = \frac{2}{3}\bar{r}\sqrt{\frac{8\,R\,T}{\pi M_{H_2O}}} \tag{5}$$

In the case of a porous medium such as stone having a large distribution of pore diameters, with some pores wider and some narrower than the mean free path ($0.01 < N_K < 10$), an estimate can be made of the diffusivity using the Dusty Gas Model (Mason, 1983)

$$\frac{1}{D_t} = \frac{1}{D_m} + \frac{1}{D_K} \tag{6}$$

Here D_t is the diffusivity in the transition regime between Knudsen and molecular diffusion. At standard temperature and pressure, λ, the mean free path of water molecules diffusing through the air contained in the pores is 8.63×10^{-8} m (Perry and Chilton, 1973).

While Dolomitican marble and Pietra Serena sandstone have average pore radii in the tenths of microns (0.13 and 0.3 μm, respectively) Pietra di Lecce limestone has an average pore radius in the μm range (1.1 μm) (Table 1). Another important difference between these three lithotypes is their average porosity: 0.5% for marble, 9.2% for sandstone, and 32% for limestone. The bulk of the pore radii distribution in each lithotype are in the range from 0.01 micron to 2 microns (Hénon, 1999). The values of N_K for this pore radius range are between 0.1 and 10, which means that the diffusion taking place in these samples mostly occurs in the transitory mode. The diffusion coefficient D used in Eq. 2 was therefore taken to be equal to the transitory diffusion coefficient D_t. The resulting diffusion coefficients for the different regimes and the different stones used in this analysis are reported in Table 2.

Table 1. Characteristics of Marble, Sandstone, and Limestone Samples

Stone Type	Dolomitican Marble	Pietra Serena Sandstone	Pietra di Lecce Limestone
Chemical composition	100% Dolomite	32% Quartz 21% Calcium carbonate 13% Plagioclasi 7% Ortoclasio 7% Dolomite 20% Other	95% Calcite 5% Argileous minerals
Pore radius (μm)	0.13 ± 0.05	0.3 ± 0.1	1.1 ± 0.3
Porosity (%)	0.5 ± 0.10	9.2 ± 0.2	32.0 ± 2.0

Diffusion in the coated stone

The effective diffusivity of water vapor in natural (uncoated) stone is denoted by $D_{0,\text{eff}}$. When a polymeric coating is applied on the stone surface and penetrates the porous

Table 2. Water-Vapor Diffusion Coefficient in the Marble, Sandstone, and Limestone

	D_m (molecular) (cm^2/s)*	D_K (Knudsen) (cm^2/s)**	D_t (Transitory) (cm^2/s)†
Marble	0.26	0.513	0.173
Sandstone	0.26	1.184	0.213
Limestone	0.26	4.341	0.245

*Geankoplis, 1993.
**Equation 5 (Geankoplis, 1993).
†Equation 6 (Mason, 1983).

medium to a depth δ (Figure 2), the effective diffusion coefficient of water vapor in this coated region is modified and referred to as $D_{1,\text{eff}}$. The overall effective diffusivity of the coated stone, $\overline{D}_{\text{eff}}$, is the result of the effective diffusivity in the coated layer of thickness δ, $D_{1,\text{eff}}$ and the effective diffusivity in the noncoated layer of thickness L-δ, $D_{0,\text{eff}}$. Because at steady state the molar flux of water vapor diffusing through the stone sample is constant in the direction of flow, integration of Eq. 1 from one end of the sample to the other results in

$$c_1 - c_0 = <J> \int_0^L \frac{dx}{D_{\text{eff}}(x)} = <J> \frac{L}{\overline{D}_{\text{eff}}} \tag{7}$$

where c_1 is the solute molar concentration at $x = 0$, c_0 is the solute molar concentration at $x = L$, and $\overline{D}_{\text{eff}}$ is the average effective diffusivity for the coated sample. Breaking up the integral into contributions from the coated and the uncoated layers, Eq. 7 can be written in the form

$$c_1 - c_0 = <J> \left[\int_0^{L-\delta} \frac{dx}{D_{\text{eff}}(x)} + \int_{L-\delta}^{L} \frac{dx}{D_{\text{eff}}(x)} \right] = <J> \frac{L}{\overline{D}_{\text{eff}}} \tag{8}$$

Recalling that $D_{\text{eff}}(x)$ is equal to $D_{0,\text{eff}}$ from 0 to L-δ and equal to $D_{1,\text{eff}}$ from L-δ to L, Eq. 8 leads to

$$\frac{D_{0,\text{eff}}}{D_{\text{eff}}} = 1 + \left(\frac{\delta}{L}\right)\left(\frac{D_{0,\text{eff}}}{D_{1,\text{eff}}} - 1\right) \tag{9}$$

Using Eq. 2, and assuming that the tortuosity in the noncoated and the coated zones are equal, one can write

$$D_{0,\text{eff}} = \frac{\epsilon_0}{\tau} D_0 \tag{10}$$

and

$$D_{1,\text{eff}} = \frac{\epsilon_1}{\tau} D_1 \tag{11}$$

where ϵ_0 and ϵ_1 are, respectively, the porosity in the noncoated layer and the porosity in the coated layer of the stone sample.

For diffusion in the transition regime, the ratio of the effective diffusivities in the uncoated and coated layers is proportional to the pore volume fraction in those regions multiplied by the ratio of the transitory diffusion coefficient in the uncoated and the coated layers

$$\frac{D_{0,\text{eff}}}{D_{1,\text{eff}}} = \left(\frac{\epsilon_0}{\epsilon_1}\right) \frac{D_{0,t}}{D_{1,t}} \tag{12}$$

where, using Eq. 6

$$\frac{D_{0,t}}{D_{1,t}} = \frac{D_{K,0}}{D_{K,1}} \left(\frac{1 + D_{K,1}/D_m}{1 + D_{K,0}/D_m} \right) \tag{13}$$

According to Eq. 5, the ratio of the Knudsen diffusion coefficients in the two layers is proportional to the ratio of the pore radii in each layer

$$\frac{D_{K,0}}{D_{K,1}} = \frac{\bar{r}_0}{\bar{r}_1} \tag{14}$$

Here $\bar{r}_0$ is the average pore radius before coating, and $\bar{r}_1$ is the average radius of the pores in the coated layer. If the pores are coated by polymer, the average pore radius available for water-vapor transport, $\bar{r}_1$, should be smaller than the initial pore radius, $\bar{r}_0$. As a first approximation it can be assumed that the pores have a cylindrical shape, and that once applied on the stone surface the polymer is distributed as a layer on the pore walls, making it possible to relate the change in porosity to the change in the pore radius

$$\frac{\epsilon_0}{\epsilon_1} = \frac{\text{Pore volume before coating}}{\text{Pore volume after coating}} = \frac{\pi \bar{r}_0^2 L}{\pi \bar{r}_1^2 L} = \left(\frac{\bar{r}_0}{\bar{r}_1}\right)^2 \tag{15}$$

By substituting Eq. 15 into Eqs. 14, 13 and 12, the ratio of diffusivities in uncoated and coated layers becomes

$$\frac{D_{0,\text{eff}}}{D_{1,\text{eff}}} = \left(\frac{\epsilon_0}{\epsilon_1}\right)^{3/2} \left(\frac{1 + D_{K,1}/D_m}{1 + D_{K,0}/D_m} \right) \tag{16}$$

and the general equation relating the overall effective diffusivity to the local diffusivities (Eq. 9) takes the form

$$\frac{D_{0,\text{eff}}}{D_{\text{eff}}} = 1 + \left(\frac{\delta}{L}\right) \left[\left(\frac{1 + D_{K,1}/D_m}{1 + D_{K,0}/D_m} \right) \left(\frac{\epsilon_0}{\epsilon_1}\right)^{3/2} - 1 \right] \tag{17}$$

The porosity, ϵ_1, which is not easily measurable, can be estimated as being the pore volume remaining in the coated layer after the coating process, divided by the total volume of the coated region of the stone. Assuming that all the polymer applied on the stone surface penetrates inside the pores of the substrate, the porosity difference between the uncoated and the coated regions can be estimated as being equal to the volume of polymer, V_p, deposited on the sample surface, divided by the total volume of the coated layer, δA, where A is the area of the top surface of the stone sample

$$\epsilon_0 - \epsilon_1 = \frac{V_p}{A\delta} \tag{18}$$

Since $V_p = M_p/\rho_p$, where M_p and ρ_p are, respectively, the mass and the density of the polymer applied, Eq. 18 is equiv-

alent to

$$\frac{\epsilon_1}{\epsilon_0} = 1 - \frac{M_p/A}{\rho_p \delta \epsilon_0} \tag{19}$$

By substituting this result in Eq. 17, we obtain an equation for δ, in which M_p/A can be measured, ρ_p is a known polymer property, $D_{0,\text{eff}}$ is the measured overall effective diffusivity of the uncoated stone, and $\overline{D}_{\text{eff}}$ is the measured overall effective diffusivity of the coated stone. The penetration depth, δ, of the polymer into the porous medium can then be estimated from Eq. 17.

Experimental Section

Stone samples

The materials examined in this study are three calcareous stones: Dolomitican marble, Pietra Serena sandstone, and Pietra di Lecce limestone. The samples used for the diffusion experiments were 1 cm thick with square cross section of 5 cm × 5 cm. All the samples of the same lithotype were taken from one large boulder, in order to minimize differences in physical properties. These samples were characterized by the Italian National Research Center of Florence (CNR-C.S. Cause Deperimento e Metodi di Conservazione Opere d'Arte, Italy); the characteristics are reported in Table 1. In this study we analyzed 9 samples of Dolomitican marble, 15 samples of Pietra Serena sandstone, and 10 samples of Pietra di Lecce limestone. Each polymer studied was applied in different amounts on several samples of the same stone type.

Polymeric material

Samples were coated with three different fluorinated polymers that had been investigated for stone protection purposes (Frediani et al., 1982; Piacenti et al., 1993). These polymers referred to as IBAo, IBA1, two perfluoropolyethers with isobutyl amides, and DC2Ao, a perfluoropolyether with an ethylene diamide were also provided by the CNR of Florence, Italy. The chemical formulas of these polymers, together with their density, viscosity, and average molecular weights, are reported in Table 3.

Coating process

These polymers were dissolved in carbon dioxide at a weight concentration of about 1%, a solution temperature of 40°C, and a solution pressure of 275 bar. The solution was then expanded through a pinhole of 100 microns in diameter (RESS process) using the spraying device shown in Figure 3. To compensate for the temperature drop of the solution at the nozzle, the nozzle tip was heated to 100°C. During the expansion of the polymeric solution through the nozzle, a rapid supersaturation of the solute was obtained, producing a fairly even polymeric coating on the stone substrate. The substrate was placed at a distance of about 10 cm from the nozzle tip, and the spraying time ranged between a few seconds and 3 min, according to the surface coverage of polymer desired on the stone substrate. The mass of polymer per surface area received by each sample was measured by weight difference before and after coating. No efforts were made to optimize the transfer efficiency of polymer to the stone samples. There were significant losses of polymer, probably more than 60%, as a result of aerosol formation at the nozzle tip. Prior to being coated, the samples were taken out of an oven where they were constantly kept at 45°C, and were placed in a desiccator [relative humidity (RH) < 10%], where they cooled for 2 h to ambient temperature. The samples were then weighed and the masses recorded for later use. The average mass of a 25-cm^3 sample was about 70 g for marble, 62 g for sandstone, and 42 g for limestone. Once coated, the samples were placed back in the oven. After several days in the oven and 2 h of cooling in the desiccator, the samples were weighed one more time. The weight difference between an uncoated and a coated sample corresponded to the mass of coating applied on the sample surface. Accuracy in the measurements was approximately ± 0.5 g/m^2 ($1.25\ 10^{-3}$ g/25 cm^2). The stone surfaces coated with polymer were allowed time for polymer penetration into the pores prior to measurement of water ab-

Table 3. Chemical Formula and Physical Properties of Polymers Investigated

Abbreviation	Formula	State
YR	CF_3—O—Rf—CF_3	Oil
IBAG2200 (IBAo)	CF_3—O—Rf—CF_2—CO—NH—CH_2—CH—$(CH_3)_2$	Oil
IBA1	40% IBAG2200 / 60% YR	Oil
DC2G2200 (DC2Ao)	CF_3—O—Rf—CF_2—CO—NH—$(CH_2)_2$—NH —CO—CF_2—O—Rf—CF_3	Oil
—Rf—	—$[CF_2$—$CF(CF_3)$—$O]_m$—$[CF_2$—$O]_n$—	

Abbreviation	$d^4_{25°C}$* (g/mL)	Vis. at 20°C** (cSt)	Avg. MW (g/mol)
YR	1.894	1,597	6.500†
IBAG2200 (IBAo)	1.822	1,008	2.280††
IBA1	1.839	330	N.A.
DC2G2200 (DC2Ao)	1.880	43,362	4,485††

*$d^4_{25°C}$ is the density of the polymer and is numerically equal to the ratio of the density of that liquid at $T = 25°C$ and of the density of water at $T = 3.98°C$ (~ 4°C).

**The viscosity values were obtained with a Cannon Fenske capillary viscometer (Piacenti and Camaiti, 1994).

†Average molecular weight (MW) was measured by ^{19}FNMR (Pianca et al., 1995).

††Average molecular weight (MW) was measured by vapor pressure osmometry (Wescan osmometer model 233) in 1,1,2-trichlorotrifluoroethane solution (Piacenti and Camaiti, 1994).

sorption or water-vapor diffusion. It was not possible to measure the film thickness of the polymer on the surface because the thin films formed (probably on the order of 0.1–0.5 μm) and the rough nature of the surface. The coating was made uniform throughout the stone surface by moving the sample below the nozzle during spraying.

Liquid water absorption

The reduction in liquid water absorption due to a coating is sometimes defined in the literature as the "protective efficacy" of the polymeric material (Doc NORMAL 11/85, 1985). This protective efficacy (PE) is defined as

$$PE = \frac{m_o - m_1}{m_o} \cdot 100\ (\%) \tag{20}$$

where m_o and m_1 are, respectively, the mass of water absorbed by the sample before and after it has been coated. The experiment consisted of placing stacks of 20 paper filters (9 cm diameter) in a glass baking dish, filled with approximately 1 cm of dionized water (the water level should be below the height of the stack of paper filter in order for them to get wet by capillary absorption). When the paper filters were completely damp, the stone samples were taken out of the desiccator, weighed, and always placed horizontally on a filter stack, the face to be treated in direct contact with the damp filter. After one hour for the marble and sandstone and 20 min for the limestone, the samples were removed from the baking plate, slightly dabbed with a damp piece of chamois skin, and weighed again. The increase in weight corresponded to the water absorbed by capillarity. Each measurement was repeated at least three times with intervals of a couple of days, during which the samples were placed back in the oven at 45°C, to allow the absorbed water to evaporate from the stone sample. This experiment was also repeated on the coated stone samples, and the protective efficacy of the protective material was calculated. Experimental results of liquid water absorption are given in Figure 1.

Water-vapor diffusion

The device used to measure the water-vapor flux through the stone substrates is illustrated in Figure 4, and is similar to others found in the literature (Doc NORMAL 21/85, 1985). The main body consisted of a cylindrical Plexiglas cell of 10.5-cm OD and 7 cm in height. A cylindrical reservoir 4 cm in diameter and 2.8 cm deep holds liquid water while a receptacle of $5 \times 5 \times 1.5$ cm, carved directly above the reservoir held the stone sample horizontally. Rubber gaskets (silicon rubber of 4.0 durometers) were placed under and above the stone to prevent the water vapor from detouring around the sample. The lid of the device was made out of oxidized alu-

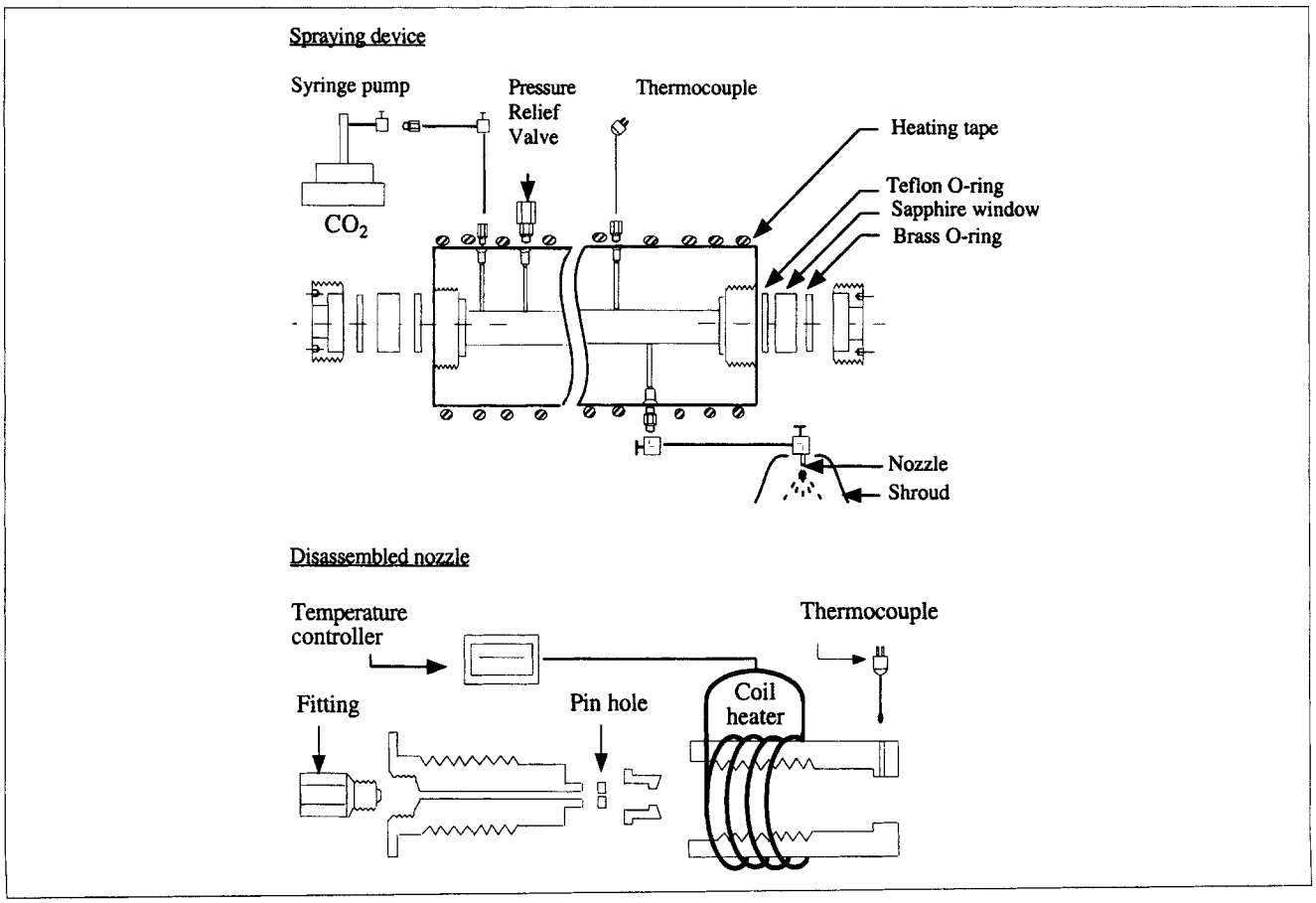

Figure 3. Spraying device and nozzle details.

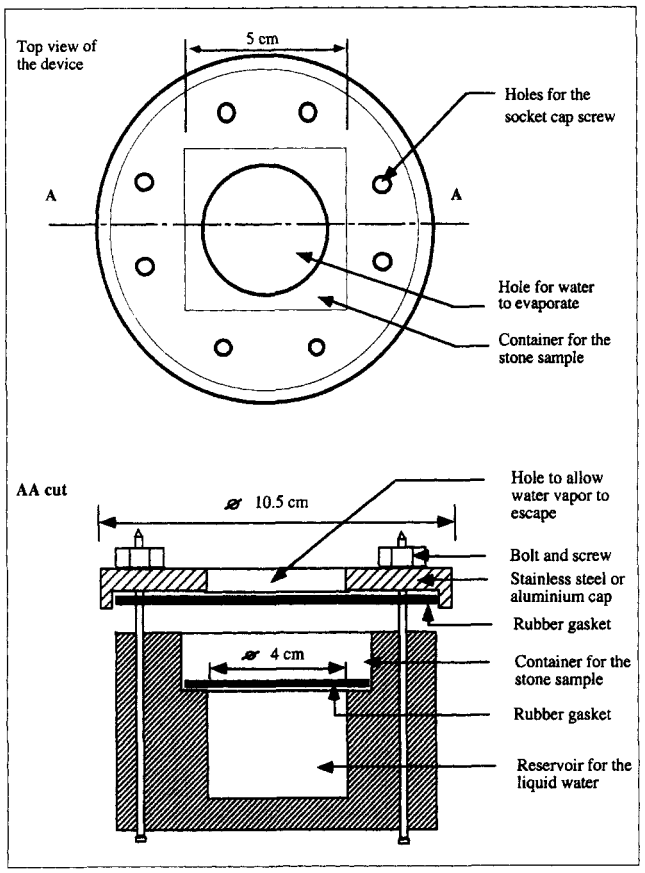

Figure 4. Diffusion device.

minum, with a 4-cm-dia. hole in the middle, to allow the water contained in the reservoir to evaporate. The two sections of the device were tightened uniformly with bolts.

The diffusion devices were placed in a glove box. The RH of the air inside the box was kept low (RH of ~ 14%) by distributing desiccant (~ 500 g of calcium sulfate) in several trays inside the environmental chamber. The box was insulated on all sides except for the glove door, to maintain a constant inside temperature of about 25°C. A high-precision balance (Mettler-Toledo-Model PR 1203) was also kept in the conditioned space. The length of the experiment was about three weeks, during which the weight of each cell was recorded daily. The weight loss of a given cell corresponds to the amount of liquid water evaporated through the porous stone sample.

The molar flux $< J >$ of water vapor diffusing through the stone sample can be related to the rate of weight loss of the liquid water contained in the reservoir

$$< J > = \frac{\text{mols}_{H_2O}}{\text{Area} \cdot \text{time}} = -\frac{1}{A}\frac{1}{M_{H_2O}}\frac{dW_{H_2O}}{dt} \qquad (21)$$

where W_{H_2O} is the weight of water, M_{H_2O} its molecular weight, and A the area available for the diffusion process. Substituting Eq. 21 into Eq. 1, one obtains an expression used to compute D_{eff} (D_{eff} being $D_{0,\text{eff}}$ if the stone is uncoated and $\bar{D}_{\text{eff}}$ if the sample has received a polymeric coating)

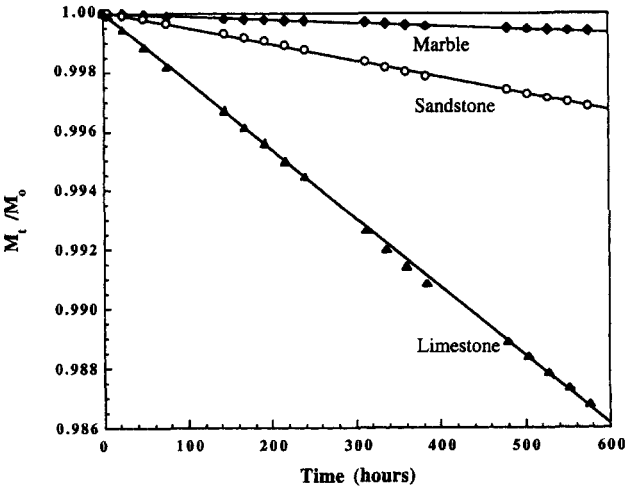

Figure 5. Typical water mass evaporation rates in natural marble, sandstone, and limestone samples (M104, S104, and L104 uncoated).

$$< J > = -\frac{1}{A}\frac{1}{M_{H_2O}}\frac{dW_{H_2O}}{dt} = D_{\text{eff}}\left[\frac{c_1 - c_0}{L}\right]$$

$$= \frac{D_{\text{eff}}}{RT}\left[\frac{p_1 - p_0}{L}\right] \qquad (22)$$

Here the molar concentrations of the solute are related to the partial pressures through the ideal gas law. The quantities p_1 and p_0 are the partial pressures of water inside and outside the cell and are known parameters. The pressure p_1 is equal to 23.756 mmHg, corresponding to the pressure of saturated water vapor at the box average temperature of 25°C, while p_0 is taken to be equal to 14% of the saturated vapor pressure, due to the 14% relative humidity generally present in the box. The rate of water loss in the reservoir, dW_{H_2O}/dt, which equals the weight loss of the whole cell, is obtained from the slope of the device mass curve with time (M_t/M_o vs. t). Typical weight losses of water vapor diffusing through 12 cm^2 of uncoated 1-cm-thick stone samples were around 0.0007 g/h for marble, 0.004 g/h for sandstone, and 0.01 g/h for limestone. Bypass of water vapor around the tested samples was estimated to approach 0.0002 g/h. A typical M_t/M_o curve for each lithotype is given in Figure 5.

The penetration depth of the polymer inside the porous medium was then estimated using Eqs. 17 and 19 from the experimental values of $D_{0,\text{eff}}$ and $\bar{D}_{\text{eff}}$, as described previously.

As discussed earlier, prior to measurement of water-vapor diffusion, the stones were held in a desiccator to prevent water adsorption. The stones were then placed horizontally above the liquid-water container shown in Figure 4, with a water-vapor space between the liquid surface and the lower-stone face. Water vapor adsorbed to the stones very quickly upon exposure to this water vapor. For example, in the case of marble, our lowest porosity material, the effective diffusivity for water vapor is on the order of 8.33×10^{-4} cm^2/s. The thickness of the stone samples was 1 cm. As a result, the time scale for diffusion of water vapor through the samples was no

longer than 20 min. During that time, water vapor condensed on the smaller pores and saturated the stone. We found that in a matter of a few hours, about 7% of the pore volume of sandstone, 3% of the pore volume of marble, and 1% of the pore volume of limestone was filled with adsorbed water. These values were determined by direct measurement of the change in weight of the stones themselves.

After that time, the water vapor is basically diffusing through a porous stone whose smaller pores contain water absorbed by capillary condensation. As shown in Figure 5, our water-vapor flux experiments lasted about a month. Over this time frame the short time required for absorption of water and equilibration of the stone with the water vapor is negligible. As a result, Eqs. 21 and 22 adequately describe the phenomenon observed in Figure 5. This is a perfectly constant rate of mass flux of water out of the sample holder. Any other scenario that would include the potential accumulation of water in the stone as a result of adsorption would give rise to nonlinear mass loss vs. time results, contrary to what is shown in Figure 5. For example, if pores were completely blocked over time, the mass flux would be reduced. No such behavior was observed, and as a result, we do not believe that water absorption or accumulation leading to filling of pores was occurring.

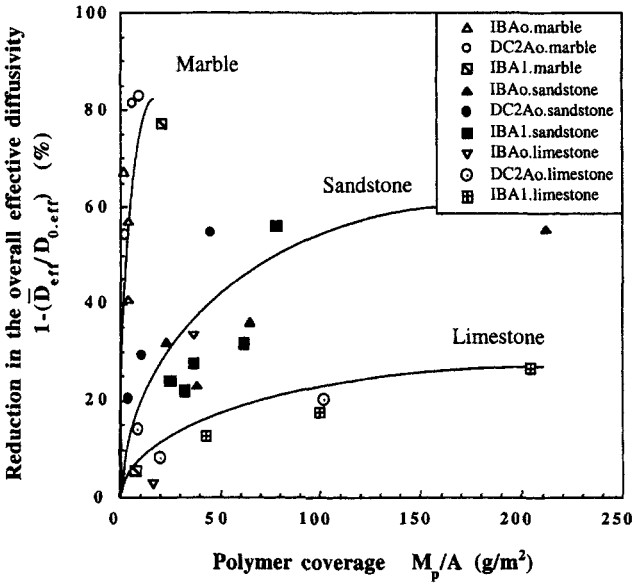

Figure 6. Reduction in the overall sample effective diffusivity as a function of polymer surface coverage.

Results and Discussion

The results of liquid water absorption (Figure 1) show that the protective efficiency of a polymeric coating varies with the nature of the substrate and the amount of polymer applied on each sample. The protective efficiency increases rapidly at low surface coverage, eventually reaching a maximum at higher coating levels. Analysis of Figure 1 reveals that for the same polymer coverage, the hydrorepellence of the diamide (DC2Ao) is higher than for the monoamide (IBA1). The presence of isobutyl terminal groups in the monoamide formula is probably responsible for this difference in protective efficiency. The hydrorepellence of the amide polymers is enhanced by the configuration of the molecule at its interface with the stone substrate. It is believed that the nitrogen of the amide binds to the stone via hydrogen bonds, while the perfluoropolyether part of the polymer is left at the interface of the coating with the outside environment. The nonpolar nature of the perfluoropolyethers renders the polymers very hydrorepellent.

The average effective diffusivities measured for noncoated samples of marble, sandstone, and limestone are 8.08 10^{-4} cm^2/s, 5.32 10^{-3} cm^2/s, and 1.87 10^{-2} cm^2/s, respectively. $D_{0,eff}$ is approximately constant from sample to sample of a given stone material, but varies considerably from one lithotype to the other. As expected from Eq. 2, the higher the stone porosity, the easier the transport of water vapor across the stone sample and the larger the effective diffusivity. The tortuosity results are also comparable from sample to sample of a given stone material. The average tortuosities calculated for each lithotype are 1.2 for marble, 3.7 for sandstone, and 4.3 for limestone. The differences in the average tortuosity values from one stone material to the other can be ascribed to the differences in microstructure between the lithotypes. While marble is a metamorphic rock, whose constitution changes by natural means like heat and pressure, sandstone and limestone are two sedimentary rocks formed by the accumulation of sediment deposition; and it seems normal that their tortuosities are higher due to the more uneven process of stone formation. In further calculations it was assumed that the tortuosity of a given stone does not vary considerably upon the application of a polymeric coating on the material surface.

Effective diffusivity values for coated stones, $\overline{D}_{eff}$, were obtained and compared to the effective diffusivities for noncoated stones. The decrease in the overall effective diffusivities is plotted in Figure 6 as a function of the polymer coverage on each substrate. The lines drawn on the plot indicate a general increase in the overall effective diffusivity reduction with an increase in the polymer coverage. From Figure 6, it is evident that for an equal amount of the same polymer, the reduction in the overall diffusivity coefficient is different for different stone materials, and increases as the porosity and the average pore radius decreases. It may also be noted that the reduction in the overall effective diffusivity coefficient is not strongly dependent on the coating material.

Using experimental values of and $D_{0,eff}$ and $\overline{D}_{eff}$, the penetration depth, δ, of the polymer into the porous medium and the porosity, ϵ_1, of the coated layer can be estimated using Eqs. 17 and 19. The effective diffusivity coefficient of water vapor in the coated layer $D_{1,eff}$ can be estimated using Eqs. 13 and 11. Figure 7 is a plot of the penetration depth of the different polymers into the different lithotypes as a function of the amount of material applied on the stone surface. For an equal surface coverage, the penetration depth in marble is higher than the one in sandstone, which is higher than the one in limestone, due to differences in the stone porosities and average pore radii.

When local properties such as ϵ_1 (Figure 8) and $D_{1,eff}$ (Figure 9) are examined, a sudden increase in the reduction of these properties is observed at low surface coverage, fol-

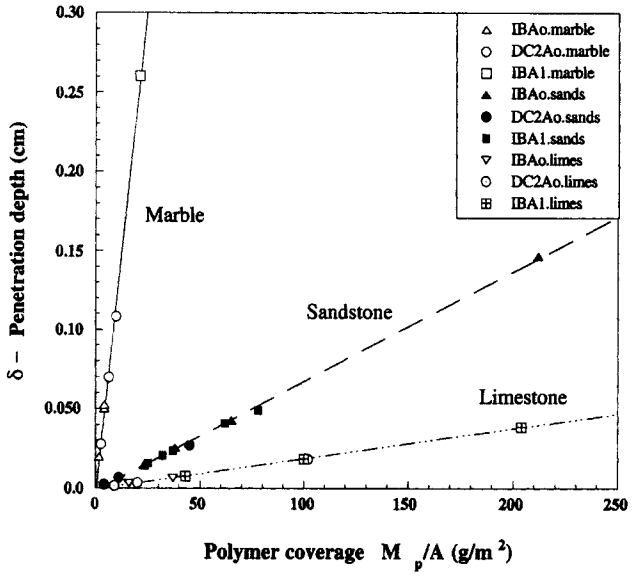

Figure 7. Polymer penetration depth as a function of polymer surface coverage.

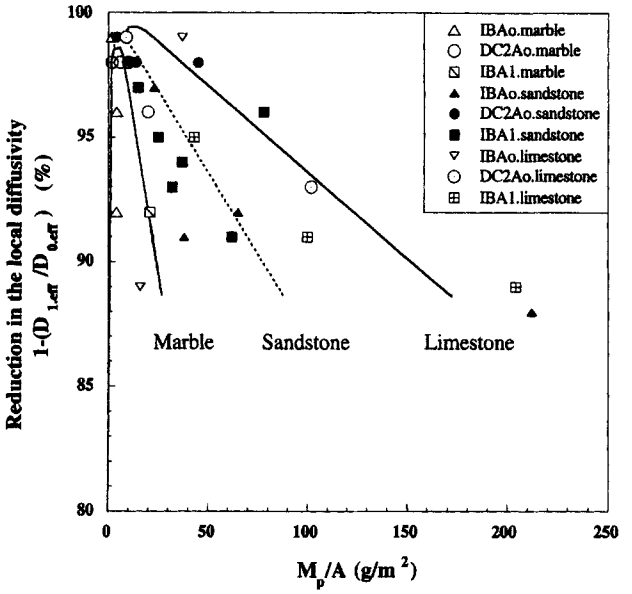

Figure 9. Reduction in the local sample diffusivity as a function of polymer surface coverage.

lowed by a maximum reduction close to 100% (for coverage around 5, 10, and 20 g/m^2, for marble, sandstone, and limestone, respectively) and a gradual decrease in the property reduction, from ~99% to 80% as the polymer coverage increases from 5/20 g/m^2 (according to the lithotype) to 250 g/m^2. To explain the decrease in pore blockage with an increase in the amount of polymer material applied on the sample, the mechanism of polymer penetration in the pores was investigated.

The initial thickness of the coating film applied on the sample surface is denoted l_0 and is equal to

$$l_0 = \frac{M_p}{A}\frac{1}{\rho_p} \tag{23}$$

A plot of the porosity reduction in the coated layer as a function of the ratio l_0/r_0, where r_0 is the average pore radius of the sample substrate, is given in Figure 10. The net collapse of the data toward a central trend indicates the importance

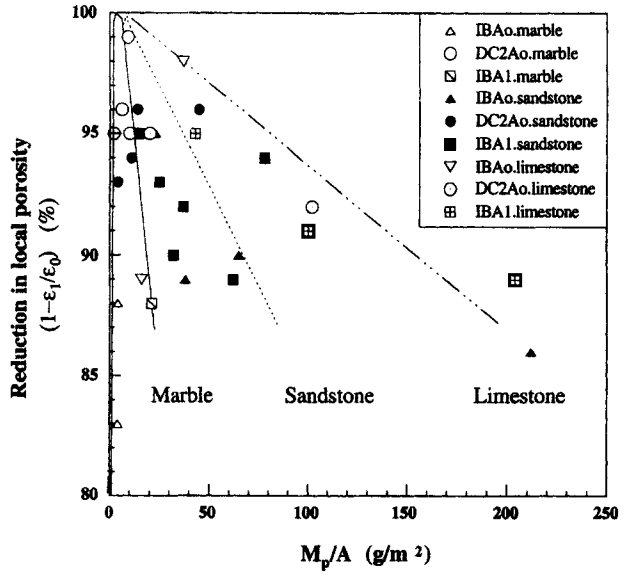

Figure 8. Reduction in the coated-layer porosity as a function of polymer surface coverage.

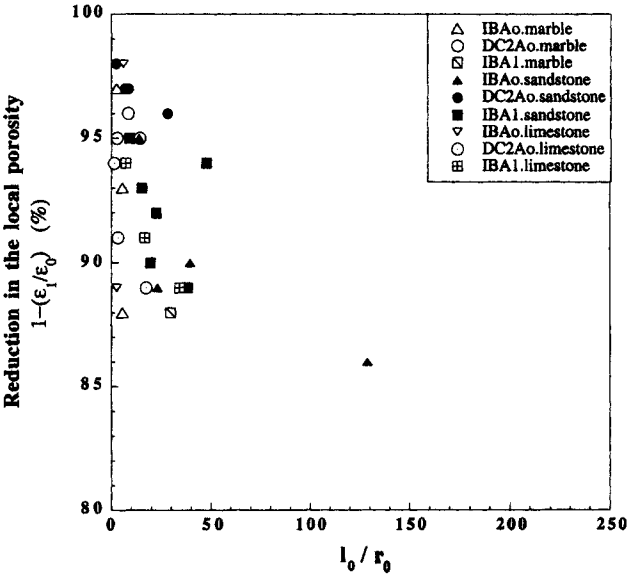

Figure 10. Reduction in the coated-layer porosity as a function of the ratio of the initial film thickness divided by the medium average pore radius.

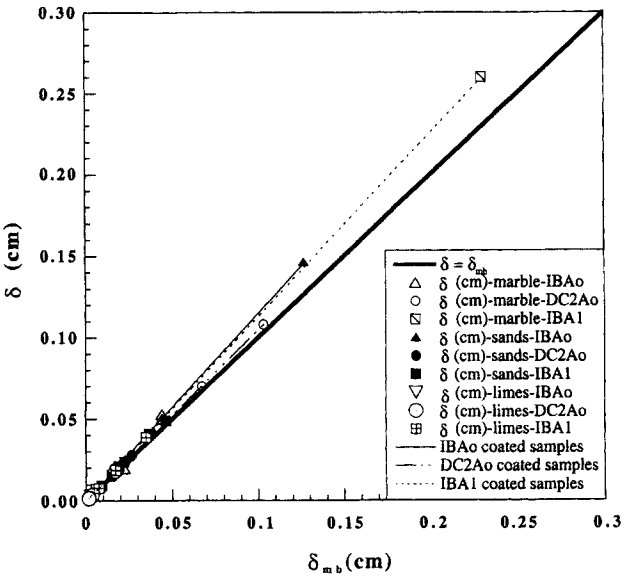

Figure 11. Diffusivity-derived penetration depth vs. mass-balance-calculated penetration depth.

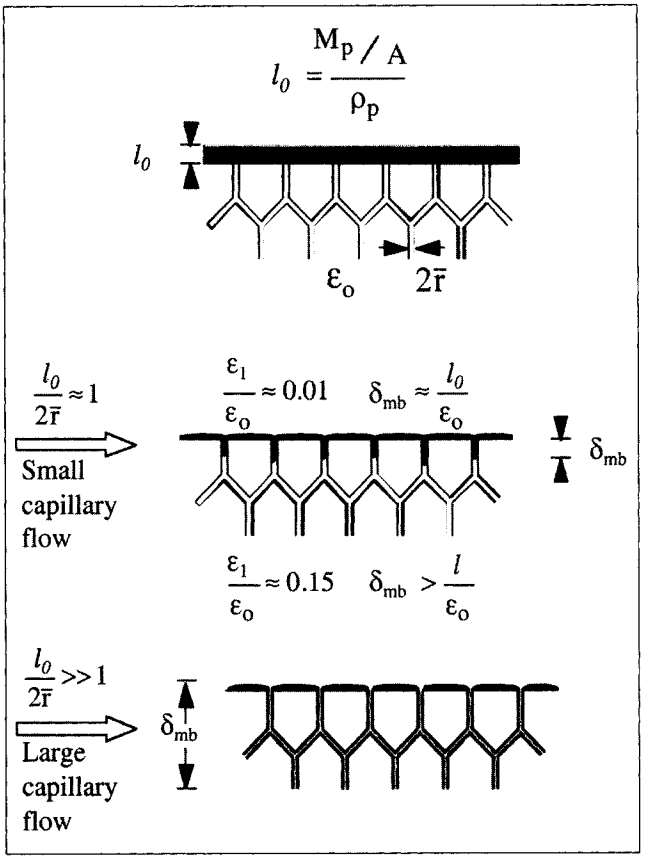

Figure 12. Penetration depth process in porous medium as a function of the surface coverage.

of the substrate pore size in the polymer penetration mechanism. Furthermore, a mass balance conducted on the polymeric film of thickness l_0 applied on a medium of porosity ϵ_0, indicates the polymer should penetrate in the pores by a depth equal to l_0/ϵ_0. We denote by δ_{mb} this penetration depth obtained by mass balance. Calculation of δ_{mb} for each sample and each surface coverage gave mass-balance penetration depths very close to the ones derived from the diffusivity experiment, δ. Figure 11 shows the variation of δ and δ_{mb} for the same surface coverage, indicating that the difference between these two values increases as the surface coverage, M_p/A, increases, with values of δ being larger than δ_{mb}. This possibly indicates that at low polymer coverage, penetration of the polymer in the pores occurs by capillary action, while at higher polymer coverage another process, such as gravity, enhances the capillary effect to give rise to larger penetration depths. Polymer penetration depth is also influenced by the internal structure of the porous medium, as shown in Figure 12. In fact, for film thicknesses smaller than the average pore radius of the substrate, δ values are equal to δ_{mb}, independently of the lithotype considered, thus independently of the initial porosity of the substrate. In this case, the polymer barely wets the pores and no particular forces act on the polymer. As l_0 increases, pore blockage increases. For film thicknesses of the same order of magnitude as the average pore radius, plugging of the pore recurs and pore blockage reaches the maximum. Finally, as l_0 becomes much larger than the average pore size of the medium, a larger driving force acts on the polymer, forcing it to penetrate deeper into the medium. Figure 11 also shows the linear fit of all the samples (marble, sandstone, and limestone) coated with the same polymer (IBAo, DC2Ao, or IBA1). The linear regression seems to indicate that for the same amount of polymer coating and independently of the substrate, the depths of penetration, δ, of the IBAo polymer are larger than the ones obtained with IBA1, which are in turn larger than the ones for DC2Ao. Although the penetration depth difference is not significant at low polymer coverage, it increases monotonically with the amount of polymer applied per surface area of the substrate. Differences in the penetration depths of the three polymers may result from their differences in viscosity, which are of 1008, 330, and 43,362 cSt for IBAo, IBA1, and DC2Ao, respectively (see Table 3).

Conclusion

The analysis of water-vapor transport rates across stone samples coated with different fluorinated polymers allowed an improved understanding of the influence of the polymeric coating on the natural properties of the stone sample as well as the process penetrating such coatings in the porous medium.

The three perfluoropolyethers studied in this article proved to be hydrorepellent, with a protective efficacy increasing with the amount of polymer applied on the sample surface. It was also verified that the presence of amide groups in the polymer molecule increases the hydrorepellence of the coating. The liquid-water absorption measurements identified the diamide perfluoropolyether, DC2Ao, as the most hydrorepellent of the three polymers investigated. It is noted that polymers delivered from a carbon dioxide solution can exhibit a hydrorepellence (protective efficiency) comparable to the polymers delivered by brush or impregnation coatings from organic solvents (Piacenti and Camaiti, 1994). Since all of the

polymers in this study are liquids at room temperature, the RESS process produces liquid droplets, not solid particles. Once the liquid droplets hit the surface, the liquid begins to penetrate the pores, ultimately forming a transparent, extremely thin film that is not apparent to the naked eye. We estimate below that the film thickness formed is on the order of 0.1 to 0.5 μm, but this is extremely hard to measure directly on a rough surface. The viscosity of the various polymers (Table 3) did not seem to play a major role in the effectiveness of the coating. Again, the results for liquid-water absorption shown here are the same as those determined by Piacenti and Camaiti (1994), using a liquid fluorocarbon applied by brush.

The water-vapor diffusion experiment allowed estimates of the polymer penetration depth and of the percentage of pore blockage as a function of polymer coverage. Penetration depths were found to be in the micron range and to increase with increasing polymer coverage and decreasing pore radius and porosity of the medium. The average pore radius was found to play a major role in the penetration-depth mechanism. Capillary action was defined as being the dominant mechanism governing the penetration of the polymeric material in the porous medium. At higher coverage, capillary action is possibly enhanced by gravitational force, which drives the polymer deeper into the stone. The depth of penetration, limited by the size of the pore radii, has also been shown to be slightly dependent on the polymer viscosity.

Acknowledgments

The authors thank Paul Yelvington for his help in the experimental section of this work, as well as the William R. Kenan Jr. Institute for Engineering, Technology, and Science at North Carolina State University for funding this research. The authors are also grateful to Prof. Franco Piacenti and Dr. Mara Camaiti of the CNR Center for the Preservation and Conservation of Monumental Works of Art in Florence, Italy, for providing stone samples and physical property data of these materials.

Notation

A = area of the stone material covered with polymer
c = water-vapor concentration
d = diameter of molecule
D = diffusion coefficient
D_m = molecular diffusion coefficient
D_K = Knudsen diffusion coefficient
D_t = transitional diffusion coefficient
D_{eff} = effective diffusion coefficient
$\overline{D}_{\text{eff}}$ = average effective diffusion coefficient
$< J >$ = flux of water vapor
L = thickness of the stone sample
l_o = thickness of sprayed polymer layer
$M_{\text{H}_2\text{O}}$ = molecular weight of water
M_p = molecular weight of polymer
M_t = mass of stone sample and water at a given time t
M_o = initial mass of stone sample and water at time 0
N = Avogadro's number
N_K = Knudsen number
p = partial pressure of water
$\bar{r}$ = average radius of a pore in the sample
R = ideal gas constant
T = absolute temperature
V_p = volume of polymer applied
$W_{\text{H}_2\text{O}}$ = weight of water

Greek letters

ϵ = porosity of the material
τ = tortuosity factor
λ = mean free path of water-vapor molecule
δ = depth of penetration of polymer
ρ_p = density of the pure polymer

Subscripts

0,1 = uncoated and coated regions within stone; low and high water-vapor pressure surfaces (Figure 2)

Literature Cited

Alessandrini, G., R. Bugini, R. Negrotti, and R. Peruzzi, "La Facade de l'Eglise de la Chartreuse de Pavie (Italie): Etudes sur les Anciens Traitements Superficiels," *Proc. Congr. Int. de Vienne sur l'Alteration et la Conservation de la Pierre*, Vol. 2, Lausanne, Switzerland, p. 853 (1985).

Amoroso, G. C., and V. Fassina, *Stone Decay and Conservation*, Elsevier, Lausanne (1983).

Bird, R. B., W. E. Stewart, and E. N. Lightfoot, *Transport Phenomena*, Wiley, New York (1960).

Blaga, A., and R. S. Yamasaki, "Weatherability of Acrylic-Based Plastics in Long-Term Outdoor Exposure," *Durability Build. Mater.*, **4**, 21 (1986).

Carbonell, R. G., J. M. DeSimone, and F. E. Hénon, "Method and Compositions for Protecting Civil Infrastructure," U.S. Patent No. 6,127,000 (Oct. 3, 2000).

Carman, P. C., "Fluid Flow Through Granular Beds," *Inst. Chem. Eng. Trans.*, **15**, 150 (1937).

Ciarallo, A., L. Festa, C. Piccioli, and M. Raniello, "Microflora Action in the Decay of Stone Monuments," *Proc. Int. Cong. on Deterioration and Conservation of Stone*, Lausanne, Switzerland, p. 607 (1985).

Danin, A., "Biogenic Weathering of Marble Monuments in Didim, Turkey, and Trajan's Column, Rome," *Water Sci. Technol.*, **27**(7–8), 557 (1993).

Doc NORMAL 11/85, *Assorbimento d'Acqua per Capillarita. Coefficiente di Assorbimento Capillare*, CNR-IRC, Comas Grafica, Roma (1985).

Doc NORMAL 21/85, *Permeabilita al Vapor d'Acqua.*, CNR-ICR, Comas Grafica, Roma (1985).

Dullien, F. A. L., *Porous Media—Fluid Transport and Pore Structure*, 2nd ed., Academic Press, San Diego, CA (1992).

Frediani, P., C. Manganelli Del Fà, U. Matteoli, and P. Tiano, "Use of the Perfluoropolyethers as Water Repellents: Study of Their Behavior on Pietra Serena, a Florentine Building Stone," *Stud. Conserv.*, **27**, 31 (1982).

Gauri, L. K., "Decay and Preservation of Stone in Modern Environment," *Environ. Geology Water Sci.*, **15**, 45 (1990).

Geankoplis, C. J., *Transport Process and Unit Operations*, 3rd ed., Simon & Schuster, New York (1993).

Ghigonetto, S., "La Conservation de la Pierre a Venise de 1969 a 1982," *Proc. Int. Congr. on Deterioration and Conservation of Stone*, Lausanne, Switzerland, p. 1073 (1985).

Hénon, F. E., "Environmentally Benign Polymer Coating Process for the Protection of Monumental Civil Infrastructures," PhD Thesis, Dept. of Chemical Engineering, North Carolina State Univ., Raleigh, NC (1999).

Hénon, F. E., R. G. Carbonell, M. Camaiti, F. Piacenti, A. Burks, and J. M. DeSimone, "Supercritical CO_2 as a Solvent for Polymeric Stone Protective Materials," *J. Supercrit. Fluids*, **15**, 173 (1999).

Imbalzano, J. F., D. N. Washburn, and P. M. Mehta, "Permeation and Stress Cracking of Fluoropolymers," *Chem. Eng.*, 105 (Jan. 1991).

Jaroszynska, D., and T. Kleps, "Thermal Degradation of Fluorocarbon Elastomers by Thermogravimetry," *J. Therm. Anal.*, **31**, 955 (1986).

Kaiser, J., "Supercritical Solvent Comes into its Own," *Science*, **274**, 2013 (1996).

Knudsen, M., *Kinetic Theory of Gases*, B. L. Worsnop, ed., Wiley, New York (1934).

Littmann, K., H. R. Sasse, S. Wagener, and H. Hocker, "Development of Polymers for the Consolidation of Natural Stone," *Proc. Conf. Conservation of Stone and Other Materials*, Vol. 2, M.-J. Thiel, ed., E&FN Spon, London, p. 681 (1993).

Loeb, L. B., *The Kinetic Theory of Gases*, 2nd ed., McGraw-Hill, New York (1934).

Mason, E. A., and A. P. Malinauskus, *Gas Transport in Porous Media: The Dusty Gas Model*, Elsevier, Amsterdam (1983).

Matteoli, U., P. Tiano, M. Camaiti, and F. Piacenti, "Perfluoropolyether Isobutylamide and Isobutylester. Performance in the Protection of Stones," *Proc. Int. Cong. on Deterioration and Conservation of Stone*, J. Ciabach, ed., Nicholas Copernicus University—Press Department, Torun, Poland, p. 509 (1988).

McHugh, M. A., and V. J. Krukonis, *Supercritical Fluid Extraction: Principles and Practice*, 2nd ed., H. Brenner, ed., Butterworth-Heinemann, Boston (1994).

Perry, R. H., and C. H. Chilton, *Chemical Engineers' Handbook*, 5th ed., Chemical Engineering Series, McGraw-Hill, New York (1973).

Piacenti, F., "Chemistry for the Conservation of the Cultural Heritage," *Sci. Total Environ.*, **143**, 113 (1994).

Piacenti, F., and M. Camaiti, "Synthesis and Characterization of Fluorinated Polyetheric Amides," *J. Fluorine Chem.*, **68**, 227 (1994).

Piacenti, F., M. Camaiti, T. Brocchi, and A. Scala, "New Developments in Perfluorinated Protective Agents for Stone," *Proc. Int. RILEM/UNESCO Cong. on Conservation of Stones and Other Materials*, Vol. 2, M.-J. Thiel, ed., E&FN Spon, London, p. 733 (1993).

Piacenti, F., M. Camaiti, T. Brocchi, and A. Scala, "Protection of Stones by Perfluoropolyethers," *Proc. Int. Cong. on Deterioration and Conservation of Stone*, Vol. 3, J. D. Rodrigues, F. Henriques, and F. T. Jeremias, eds., Laboratorio Nacional de Engenheria Civil, Lisbon, Portugal, p. 1223 (1992).

Pianca, M., N. Del Fanti, E. Barchesi, and G. Marchionni, "Characterization of Perfluoropolyethers," *Chem. Today*, **1**, 29 (1995).

Present, R. D., *Kinetic Theory of Gases*, Int. Ser. in Pure and Applied Physics, L. I. Schiff, ed., McGraw-Hill, New York (1958).

Price, C. A., *Stone Conservation, An Overview of Current Research*, A. Keys, ed., The Getty Conservation Institute, Los Angeles, CA (1996).

Reddy, M. M., S. Sherwood, and B. Doe, "Limestone and Marble Dissolution by Acid Rain," *Proc. Int. Cong. on Deterioration and Conservation of Stone*, Lausanne, Switzerland, p. 517 (1985).

Sabbioni, C., and G. Zappia, "Particle Element Characterization of Urban Monuments," *J. Aerosol Sci.*, **22** (Suppl. 1), S681 (1991).

Satterfield, C. N., and T. K. Sherwood, *The Role of Diffusion in Catalysis*, Addison-Wesley, Reading, MA (1963).

Solomon, S., R. R. Garcia, F. Sherwood, and D. J. Wuebbles, "On the Depletion of Antarctic Ozone," *Nature*, **321**, 755 (1986).

Wu, C., "Consolidating the Stone," *Sci. News*, **151**, 56 (1997).

Young, P., "Pollution-Fueled Biodeterioration Threatens Historic Stone," *Environ. Sci. Technol.*, **30**, 206 (1996).

Manuscript received Mar. 23, 2001, and revision received Sept. 21, 2001.